The Niobium Phosphate Bronze $K_{5-x}Nb_8P_5O_{34}$, a New Tunnel Structure, First Member of the Series $(K_3Nb_6P_4O_{26})_n \cdot KNb_2PO_8$

A. BENABBAS, M. M. BOREL, A. GRANDIN, A. LECLAIRE,[1]
AND B. RAVEAU

*Laboratoire de Cristallographie et Sciences des Matériaux CRISMAT,
associé au CNRS URA 1318, ISMRa, Campus 2, Université de CAEN,
boulevard du Maréchal Juin, 14032 Caen Cedex, France*

A new niobium phosphate bronze $K_{5-x}Nb_8P_5O_{34}$ has been isolated. The structure of this phase has been determined from a single crystal of composition $K_4Nb_8P_5O_{34}$ by X-ray diffraction. It crystallizes in the space group $P2/c$ with $a = 13.904$ (6) Å, $b = 6.453$ (3) Å, $c = 20.64$ (1) Å, $\beta = 125.05°$ (1). This structure consists of $[Nb_3P_2O_{13}]_\infty$ layers parallel to (100) linked through PO_4 tetrahedra and $[Nb_2O_{11}]$ units. The structural relationships between this bronze and the other members of the series $(K_3Nb_6P_4O_{26})_nKNb_2PO_8$ are discussed. Attention is drawn to the fact that for this particular $n = 1$ value two structural forms can be expected. © 1990 Academic Press, Inc.

Introduction

The recent exploration of the K–Nb–P–O system in order to synthesize anisotropic phosphate bronzes was very fruitful. Beside the bronze $KNb_3P_3O_{15}$ (*1*) whose structure is closely related to the tetragonal tungsten bronze (TTB) described by Magnéli (*2*), two other bronzes, $K_3Nb_6P_4O_{26}$ (*3*) and $K_7Nb_{14+x}P_{9-x}O_{60}$ (*4*), were isolated. The structures of the latter bronzes are basically different from the TTBs; they consist of $[Nb_3P_2O_{13}]_\infty$ layers whose geometry is closely related for both oxides so that they can be considered as the members $n = \infty$ and $n = 2$, respectively of a large series of formulation $(K_3Nb_6P_4O_{26})_n \cdot KNb_2PO_8$. Moreover, it was shown that the $[Nb_6P_4O_{26}]_\infty$ framework offers the possibility

to intercalate more than three potassium ions per formula, so that a large family of isotypic bronzes $A_{4-x}Nb_6P_4O_{26}$ (*5*) could be synthesized. These results suggested that the study of the system K–Nb–P–O was at its very beginning and that other bronzes, new members of the series, should exist. We report here on the synthesis and structure of the bronze $K_{5-x}Nb_8P_5O_{34}$ ($0 < x < 1$) which corresponds to the member $n = 1$ of this series.

Synthesis

The synthesis of the polycrystalline bronze $K_{5-x}Nb_8P_5O_{34}$ was carried out in two steps. First adequate mixtures of K_2CO_3, $H(NH_4)_2PO_4$, and Nb_2O_5 were heated up to 673 K in air in order to eliminate CO_2, H_2O, and NH_3. In a second step, the finely ground product was mixed with an appropriate

amount of niobium in an evacuated silica ampoule up to 1243 K. Under these conditions we could obtain the phase for $0 < x < 1$, but only the phase with $x = 0$, i.e., $K_5Nb_8P_5O_{34}$, provided a rigorously pure yield; for x greater than zero very little trace of other oxides were observed.

Attempts to prepare single crystals, starting from the "$K_5Nb_8P_5P_{34}$" nominal composition, were unsuccessful. Different compositions were then investigated. Dark blue single crystal could be synthesized from the nominal composition $K_5Nb_6P_3O_{22}$, using the experimental method described above. The microprobe analysis of those crystals indicates only K, Nb, and P, the ratio of which agrees with the composition $K_4Nb_8P_5O_{35}$ obtained after refinement of the crystal structure.

Determination and Refinement of the Structure

A dark crystal of composition $K_4Nb_8P_5O_{34}$ with dimensions $0.216 \times 0.120 \times 0.024$ mm was selected for the structure determination. The cell parameters reported in Table I were determined and refined by diffractometric techniques at 294 K with a least-squares refinement based upon 25 reflections with $18 \leq \theta \leq 22°$.

The systematic absences $l = 2n$ for $h0l$ are consistent with the space groups $P2/c$ (No. 13) and Pc (No. 7). The refinement was successful with the centrosymmetrical space group $P2/c$.

The data were collected on a CAD-4 Enraf Nonius diffractometer with the data collection parameters reported in Table I. The reflections were corrected for Lorentz and polarization effects; no absorption corrections were performed.

The atoms were located by the heavy atom method. First, the framework "$Nb_8P_5O_{34}$" was determined and refined. A subsequent difference synthesis allowed the potassium atoms to be localized.

The relative height of these Fourier peaks showed that the K(1) site was fully occu-

TABLE I

SUMMARY OF CRYSTAL DATA, INTENSITY MEASUREMENTS, AND STRUCTURE REFINEMENT PARAMETERS FOR $K_4Nb_8P_5O_{34}$

1. Crystal data	
Space group	$P2/c$
Cell dimensions	$a = 13.904(6)$ Å
	$b = 6.453(3)$ Å
	$c = 20.64(1)$ Å $\quad \beta = 125.05(1)°$
Volume	$V = 1516(3)$ Å^3
z	2
2. Intensity measurement	
λ (MoKα)	0.71073 Å
Scan mode	$\omega - \theta$
Scan width (°)	$0.95 + 0.35 \tan \theta$
Slit aperture (mm)	$1. + \tan \theta$
Max θ (°)	45
Standard reflections	3 measured every 3000 sec (no decay)
Reflections with $I > 3 \sigma$	5 537
μ (mm^{-1})	3.72
3. Structure solution and refinement	
Parameters refined	256
Agreement factors	$R = 0.029, R_w = 0.029$
Weighting scheme	$W = f(\sin \theta/\lambda)$
Δ/σ_{max}	0.04

TABLE II

POSITIONAL PARAMETERS AND THEIR ESTIMATED STANDARD DEVIATIONS

Atom	x	y	z	$B(A2)$
Nb(1)	0.16613(2)	−0.01720(4)	0.05406(1)	0.696(3)
Nb(2)	0.24102(2)	−0.00532(4)	0.26477(1)	0.510(3)
Nb(3)	0.53830(2)	0.77407(4)	0.35353(1)	0.664(3)
Nb(4)	0.74862(2)	0.77185(4)	0.56941(1)	0.640(3)
P(1)	0.000	0.1529(2)	0.250	0.58(1)
P(2)	0.22103(5)	0.4980(1)	0.05104(3)	0.507(9)
P(3)	0.30488(5)	0.4971(1)	0.31915(3)	0.537(9)
K(1)	0.500	0.2743(2)	0.250	2.41(3)
K(2)	0.4396(2)	0.7474(5)	0.5162(2)	3.49(5)
K(3a)	0.0092(3)	0.6430(7)	0.1360(3)	5.6(1)
K(3b)	0.0444(3)	0.504(1)	0.1279(2)	6.05(9)
K(3c)	0.0571(8)	0.6856(9)	0.3357(5)	5.2(2)
O(1)	0.000	0.000	0.000	0.96(5)
O(2)	0.1895(2)	−0.0175(4)	0.1619(1)	0.86(3)
O(3)	0.3447(2)	−0.0349(4)	0.1235(1)	0.72(3)
O(4)	0.1734(2)	−0.0525(4)	−0.0330(1)	0.78(3)
O(5)	0.1732(2)	0.2900(3)	0.0573(1)	0.86(3)
O(6)	0.1544(2)	−0.3279(3)	0.0618(1)	0.83(3)
O(7)	0.4083(2)	−0.0397(4)	0.3165(1)	0.84(3)
O(8)	0.2768(2)	0.0353(4)	0.3778(1)	0.79(3)
O(9)	0.0728(2)	0.0114(4)	0.2331(1)	0.96(3)
O(10)	0.2509(2)	0.3056(3)	0.2636(1)	0.81(3)
O(11)	0.2255(2)	−0.3129(3)	0.2733(1)	0.89(3)
O(12)	0.6055(2)	0.7849(4)	0.4697(1)	0.86(3)
O(13)	0.4290(2)	0.5329(4)	0.3404(1)	1.01(4)
O(14)	0.6475(2)	0.5147(4)	0.3830(1)	0.85(3)
O(15)	0.500	0.7214(6)	0.250	1.03(5)
O(16)	0.6910(2)	0.5382(4)	0.6059(1)	1.03(3)
O(17)	0.8020(2)	0.5173(4)	0.5308(1)	0.85(3)
O(18)	0.9181(2)	0.7127(4)	0.6770(1)	0.94(3)

pied; the K(2) site, half occupied; and the third sort of potassium is distributed over three sites in a tunnel but preferentially on K(3a).

This distribution is confirmed by the refinement of the occupancy factor of the potassium atoms which indicates that 45% of K(3) is on K(3a); 32%, on K(3b); and 23%, on K(3c).

Refinement of the atomic coordinates and their anisotropic thermal parameters led to $R = 0.029$, $R_w = 0.029$ and to the atomic parameters of Table II.[2]

[2] List of structure factors and anisotropic thermal motion parameters are available on request to the authors.

Description of the Structure and Discussion

The framework "$Nb_8P_5O_{34}$" is closely related to the host lattices of the bronzes $K_3Nb_6P_4O_{26}$ (3) and $K_7Nb_{14+x}P_{9-x}O_{60}$ (4) and built up from $[Nb_3P_2O_{13}]_\infty$ layers like those oxides. Thus, $K_4Nb_8P_5O_{34}$ can be considered as the member $n = 1$ of the series $(K_3Nb_6P_4O_{26})_n \cdot KNb_2PO_8$.

Figure 1 shows the similarity of the $[Nb_3P_2O_{13}]_\infty$ layers for the three bronzes. One recognizes indeed infinite chains of corner-sharing NbO_6 octahedra running along c for $K_4Nb_8P_5O_{34}$ (Fig. 1a) and $K_3Nb_6P_4O_{26}$ (Fig. 1b) and along b for $K_7Nb_{14}P_9O_{60}$ (Fig. 1c). In the three oxides the infinite chains $[NbO_3]_\infty$ are connected through single PO_4 tetrahedra. However, the geometry of the $[NbO_3]_\infty$ chains differs from one bronze to the other. One can indeed characterize those chains by a sequence of six angles O–O–O labeled A1 to A6, formed by the edges of the NbO_6 octahedra. In $K_4Nb_8P_5O_{34}$ these angles are approximately equal to "60–60–90–120–120–90"° respectively whereas one observes the sequences "60–60–90–60–60–90"° and "120–60–90–120–60–90"° for $K_7Nb_{14}P_9O_{60}$ and $K_3Nb_6P_4O_{26}$, respectively. Consequently hexagonal windows similar to those of the hexagonal tungsten bronzes and called HTB are observed in the three bronzes, but there are two sorts of such windows—HTB and H'T'B'—in $K_4Nb_8P_5O_{34}$ (Fig. 1a) and only one sort in $K_3Nb_6P_4O_{26}$ (Fig. 1b) and in $K_7Nb_{14}P_9O_{60}$ (Fig. 1c).

Moreover the bronzes $K_4Nb_8P_5O_{34}$ and $K_7Nb_{14}P_9O_{60}$ differ from $K_3Nb_6P_4O_{26}$ by the presence of hexagonal windows similar to those observed in the brown millerite structure (7) (labeled BMW on Figs. 1a–1c); this latter type of window results from the fact that in these two bronzes the $[Nb_3P_2O_{13}]_\infty$ layers are built up from $[NbPO_5]_\infty$ chains in which one PO_4 tetrahedron alternates with one NbO_6 octahedron; such chains are or-
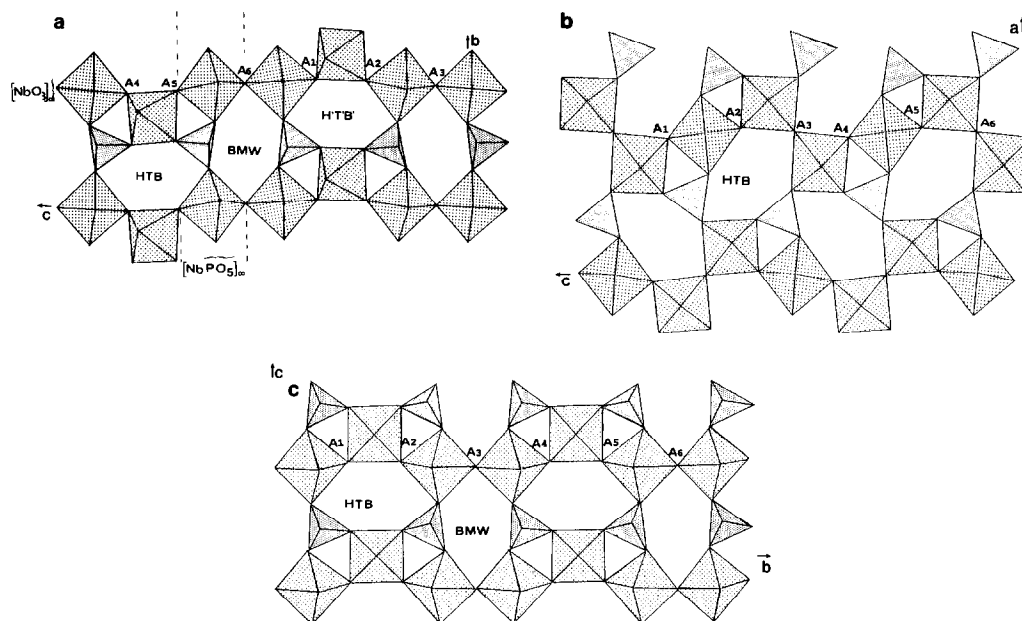
FIG. 1. $[Nb_3P_2O_{13}]_\infty$ layers in (a) $K_4Nb_8P_5O_{34}$, (b) $K_3Nb_6P_4O_{26}$, (c) $K_7Nb_{14}P_9O_{60}$.

thogonal to the $[NbO_3]_\infty$ chains, i.e., run along b in $K_4Nb_8P_5O_{34}$ (Fig. 1a) and along c in $K_7Nb_{14}P_9O_{60}$ (Fig. 1c).

The projection of the structure of K_4 $Nb_8P_5O_{34}$ along b (Fig. 2a) shows its original character with respect to the two other bronzes. This bronze can be described as

built up from $[Nb_8PO_{26}]_\infty$ layers parallel to (010) connected through planes of PO_4 tetrahedra. This framework delimits three sorts of tunnel running along b. One indeed observes five sided tunnels formed by stacking of rings of four NbO_6 octahedra and one PO_4 tetrahedron; these tunnels are closely
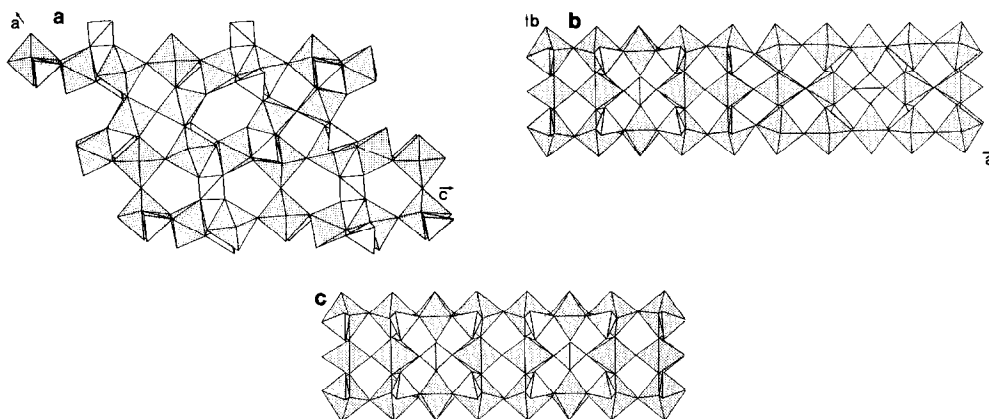
FIG. 2. Projection of (a) $K_4Nb_8P_5O_{34}$ along b, (b) $K_7Nb_{14}P_9O_{60}$ along c, (c) idealized structure of $[K_3Nb_6P_4O_{26}][KNb_2PO_8]$.

related to the pentagonal tunnels of the TTBs (2) and similar to those of $KNb_3P_3O_{15}$ (1). The second kind of tunnel consists of six-sided rings of corner-sharing octahedra similar to those observed in the hexagonal tungsten bronze (6); these tunnels differ from those of the HTBs in that the hexagonal rings do not share the corners of their octahedra along b but are linked by PO_4 tetrahedra. The third type of tunnels can be compared to those observed in the perovskite; they are built up from similar rings of four corner-sharing NbO_6 octahedra; again, here the octahedra do not share their corners along b, but are linked by PO_4 tetrahedra. It is worth pointing out that the connection of the $[Nb_8PO_{26}]_\infty$ layers with the phases of PO_4 tetrahedra leads to an important tilting of the NbO_6 octahedra within the layers. Consequently the $[Nb_8PO_{26}]_\infty$ layers are waving with respect to the (010) plane.

The comparison of the (010) projection of $K_4Nb_8P_5O_{34}$ with the (001) projection of the $K_7Nb_{14}P_9O_{60}$ (Fig. 2b) bronze shows another striking difference between these two members of the series. Both oxides are built up from $[KNb_3P_2O_{13}]_\infty$ layers, but these layers are linked to each other by $[Nb_2PO_8]_\infty$ chains running along b in $K_7Nb_{14}P_9O_{60}$, (Fig. 2b) whereas they are linked by rows of PO_4 tetrahedra and rows of double octahedral units "Nb_2O_{11}" running along c in $K_4Nb_8P_5O_{34}$.
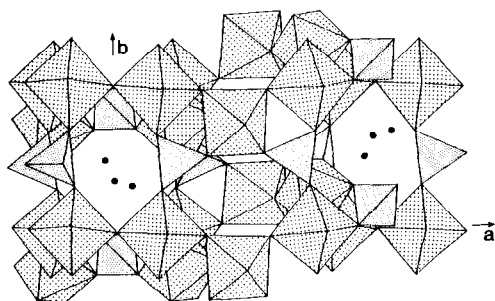

FIG. 3. Projection of the structure of $K_4Nb_8P_5O_{34}$ along c. The dots in the tunnels are the three sites over which the K(3) is distributed.

TABLE III
P–O AND Nb–O BOND LENGTHS

P(1)–O(9)	= 1.544(3) Å		
P(1)–O(9^{iv})	= 1.544(3) Å		
P(1)–O(18^{iii})	= 1.533(2) Å		
P(1)–O(18^v)	= 1.533(2) Å		
P(2)–O(5)	= 1.536(3) Å		
P(2)–O(6^{ii})	= 1.552(3) Å		
P(2)–O(14^{vi})	= 1.533(2) Å		
P(2)–O(17^{vi})	= 1.533(3) Å		
P(3)–O(10)	= 1.554(2) Å		
P(3)–O(11^{ii})	= 1.555(2) Å		
P(3)–O(13)	= 1.534(3) Å		
P(3)–O(16^{iii})	= 1.531(3) Å		
Nb(1)–O(1)	= 1.906(1) Å	Nb(3)–O(3^i)	= 1.872(2) Å
Nb(1)–O(2)	= 2.057(2) Å	Nb(3)–O(7^{ii})	= 1.926(2) Å
Nb(1)–O(3)	= 2.036(2) Å	Nb(3)–O(12)	= 2.014(2) Å
Nb(1)–O(4)	= 1.871(3) Å	Nb(3)–O(13)	= 2.082(3) Å
Nb(1)–O(5)	= 1.984(2) Å	Nb(3)–O(14)	= 2.101(2) Å
Nb(1)–O(6)	= 2.025(2) Å	Nb(3)–O(15)	= 1.913(1) Å
Nb(2)–O(2)	= 1.811(2) Å	Nb(4)–O(4^i)	= 1.990(3) Å
Nb(2)–O(7)	= 1.935(2) Å	Nb(4)–O(8^{iii})	= 1.817(3) Å
Nb(2)–O(8)	= 2.105(2) Å	Nb(4)–O(12)	= 1.870(2) Å
Nb(2)–O(9)	= 2.038(2) Å	Nb(4)–O(16)	= 2.044(3) Å
Nb(2)–O(10)	= 2.012(2) Å	Nb(4)–O(17)	= 2.136(3) Å
Nb(2)–O(11)	= 2.015(2) Å	Nb(4)–O(18)	= 2.149(2) Å

Note. Symmetry code—i: $1 - x$, $1 + y$, $0.5 - z$; ii: x, $1 + y$, z; iii: $1 - x$, $1 - y$, $1 - z$; iv: $-x$, y, $0.5 - z$; v: $x - 1$, $1 + y$, $z - 0.5$; vi: $1 - x$, y, $0.5 - z$; vii: $-x$, $1 - y$, $-z$; viii: x, $1 - y$, $0.5 + z$; ix: $-x$, $1 + y$, $0.5 - z$.

Consequently the bronze $K_4Nb_8P_5O_{34}$, that we describe as the first member of the series $(K_3Nb_6P_4O_{26})_n \cdot KNb_2PO_8$ should better be described by the formulation $(K_3Nb_6P_4O_{26}) \cdot [K(Nb_2O_6)(PO_2)]$. The idealized structure of the first member $(K_3Nb_6P_4O_{26}) \cdot KNb_2PO_8$ should indeed be built up from double $[KNb_3P_2O_{13}]_\infty$ layers connected by $[Nb_2PO_8]_\infty$ chains as shown on Fig. 2c. Thus, the existence of a second form of $K_4Nb_8P_5O_{34}$ can be expected.

The projection of the structure of $K_4Nb_8P_5O_{34}$ along c (Fig. 3) shows also a great similarity with the projection of the structure of $K_7Nb_{14}P_9O_{60}$ along a (Fig. 1a). We can indeed recognize in both structures similar brown millerite windows and hexagonal tungsten bronzes (HTB) windows. However, the different stacking of the layers along a and c in the two structures makes that one observes BMT tunnels running

TABLE IV
MAIN K–O DISTANCES

K(1)–O(3)	= 2.998(2) Å
K(1)–O(3ⁱ)	= 2.998(2) Å
K(1)–O(7)	= 3.103(3) Å
K(1)–O(7ⁱ)	= 3.103(3) Å
K(1)–O(13)	= 3.060(3) Å
K(1)–O(13ⁱ)	= 3.060(3) Å
K(1)–O(14)	= 2.772(2) Å
K(1)–O(14ⁱ)	= 2.772(2) Å
K(1)–O(15)	= 2.886(4) Å
K(1)–O(15ⁱ)	= 2.886(4) Å
K(2)–O(8ⁱⁱ)	= 3.050(3) Å
K(2)–O(12)	= 2.972(5) Å
K(2)–O(13ⁱⁱⁱ)	= 3.026(4) Å
K(2)–O(16)	= 3.167(4) Å
K(2)–O(16ⁱⁱⁱ)	= 2.790(4) Å
K(3a)–O(2ⁱⁱ)	= 3.136(5) Å
K(3a)–O(5ᵛⁱⁱ)	= 3.303(4) Å
K(3a)–O(6ⁱⁱ)	= 3.163(7) Å
K(3a)–O(9ⁱⁱ)	= 2.900(5) Å
K(3a)–O(11ⁱⁱ)	= 2.714(4) Å
K(3a)–O(17ᵛ)	= 2.627(4) Å
K(3a)–O(18ᵛ)	= 2.969(6) Å
K(3b)–O(5)	= 3.200(6) Å
K(3b)–O(6ⁱⁱ)	= 2.788(6) Å
K(3b)–O(10)	= 2.913(4) Å
K(3b)–O(11ⁱⁱ)	= 2.841(4) Å
K(3b)–O(17ᵛ)	= 2.763(4) Å
K(3b)–O(18ᵛ)	= 2.846(6) Å
K(3c)–O(4ᵛⁱⁱⁱ)	= 3.246(7) Å
K(3c)–O(9ⁱⁱ)	= 3.079(10) Å
K(3c)–O(9ⁱˣ)	= 2.598(7) Å
K(3c)–O(11ⁱⁱ)	= 3.26(1) Å
K(3c)–O(16ⁱⁱⁱ)	= 3.31(1) Å
K(3c)–O(17ⁱⁱⁱ)	= 2.636(7) Å
K(3c)–O(18ⁱⁱⁱ)	= 2.626(7) Å

Note. See footnote to Table III.

along c in $K_4Nb_8P_5O_{34}$ (Fig. 3) and HTB running along a in $K_4Nb_{14}P_9O_{60}$ (Fig. 1c).

The PO_4 tetrahedra are almost regular as in many monophosphates (Table III). The NbO_6 octahedra are very distorted with O–Nb–O angles ranging from 78.1 to 100.3° and O–O distances ranging from 2.636 to 2.173 Å (Table III). The niobium atoms have a mixed valency Nb(IV)–Nb(V) with a mean value of 4.875. The mean Nb–O bond

lengths are almost the same in the four independent NbO_6 octahedra in agreement with the delocalization of the electrons all over the niobium–oxygen ribbons.

The K(1) atoms are located in the four-sided tunnels, i.e., lie in a cage similar to that of a perovskite and are surrounded by 10 nearest oxygen atoms, with K–O distances ranging from 2.77 to 3.10 Å (Table IV). The hexagonal tunnels running along b are half occupied by K(2) atoms; in those tunnels each potassium has only five nearest neighbors, characterized by four long K–O distances ranging from 2.97 to 3.05 Å, and one shorter distance of 2.79 Å (Table IV). The third potassium ion K(3) is distributed over three sites which are located at the intersection of the pentagonal tunnels running along b and of the brown millerite tunnels running along c. In those sites, one observes seven, six, and eight neighbors for K(3a), K(3b), and K(3c), respectively. These sites are too close to each other to be completely occupied simultaneously; the occupancy factors observed here correspond to the maximum occupation of the tunnels.

These results confirm the great ability of niobium to form phosphate bronzes. The investigation of the electron transport properties of these materials are in progress.

References

1. A. LECLAIRE, M. M. BOREL, A. GRANDIN, AND B. RAVEAU, *J. Solid State Chem.* **80**, 12 (1989).
2. A. MAGNELI, *Ark. Kem.* **1**, 213 and 269 (1949).
3. A. BENABBAS, M. M. BOREL, A. GRANDIN, A. LECLAIRE, AND B. RAVEAU, *J. Solid State Chem.* **84**, 365 (1990).
4. A. LECLAIRE, A. BENABBAS, M. M. BOREL, A. GRANDIN, AND B. RAVEAU, *J. Solid State Chem.* **83**, 245 (1989).
5. M. M. BOREL, A. GRANDIN, A. BENABBAS, A. LECLAIRE, AND B. RAVEAU, *Mater. Res. Bull.* **24**, 1485 (1989).
6. A. MAGNELI, *Acta Chem. Scand.* **7**, 315 (1953).
7. E. F. BERTAUT, P. BLUM, AND A. SAGUIERE, *Acta Crystallogr.* **12**, 199 (1959).